Conducting Metallopolymers Based on Azaferrocene†

Paul D. Byrne, Peter Müller, and Timothy M. Swager*

Institute for Soldier Nanotechnologies and Department of Chemistry, Massachusetts Institute of Technology, 77 Massachusetts Avenue, Cambridge, Massachusetts 02139

Received April 20, 2006. In Final Form: June 22, 2006

A series of 2,5-thiophene-substituted 1′,2′,3′,4′,5′-pentamethylazaferrocene complexes were synthesized and electropolymerized to produce polymers with fully π-conjugated backbones. The length and hence oxidation potential of the conjugated linker (the thiophene fragments) between the metal centers were varied to understand the influence of the metal−metal interactions on the overall electroactivity of the resulting polymer. These complexes were electrochemically polymerized, and the resulting polymers were characterized by cyclic voltammetry, in situ conductivity, and spectroelectrochemistry measurements. The iron-centered oxidations significantly increased the conductivity of the polymer. The results reveal that shorter conjugated linkers cause the onset of conductivity to occur at lower potentials. This effect implies that a superexchange mechanism is likely operative in the charge migration of these polymers.

Introduction

A central issue in the development of conducting metallopolymers is the nature of the interactions of the metal centers with the conducting organic polymer backbone and how the interactions between the associated metal centers affect the overall bulk conductive properties of the polymer.[1] Understanding these interactions is a continuing focus of our research in conducting metallopolymers for sensing applications.[2] In describing the metal−polymer interactions, conducting metallopolymers can be divided into groups analogous to outer/inner sphere electron transfer in inorganic reactions between coordination complexes,[3] with the electron transfer being between the metal and the conducting organic polymer.[4] The basic distinction between the two groups is the degree of interaction between the metal and the organic π systems: indirect communication between the π electrons of the conducting polymer and the metal is labeled as outer sphere. This group comprises conducting metallopolymers where the metal is linked to the polymer chain through a non-π-conjugated linker. Direct communication between the π electrons of the conducting polymer and the metal is labeled as inner sphere. This group comprises conducting metallopolymers with the metal bound to the polymer chain by a π-conjugated linker, the metal inserted into the polymer main chain, or the metal bound directly to the polymer chain. Wolf made similar distinctions between conducting metallopolymers, but his analogy categorized conducting metallopolymers using Robin and Day's classification of mixed-valence complexes.[5] Pickup has grouped conducting metallopolymers by distinguishing between the types of interactions that occur between metal centers.[6] Our interest is focused on inner sphere-type conducting metallopolymers because these polymers display significant redox conductivity.[4,7]

A type of inner sphere conducting metallopolymer that has not been fully explored is that in which the metal is bound to the delocalized π orbitals in a *fully* π-conjugated conducting polymer. Chemical intuition would suggest that a metal bound in a π fashion should provide excellent communication between the metal and extended π-electron system of the polymers.[8,9] Although there are multiple conducting metallopolymers with a fully π-conjugated backbone wherein the metal is bound through σ bonds, there are few examples of transition metals bound in a π fashion.[10] The majority of conducting metallopolymers with π-bound metals are based upon the 1,1′-substituted ferrocene structure.[1,11] With 1,1′-substitution, the π-conjugated organic polymer segments are physically separated by the Fe center. This architecture produces polymers with a physically segmented structure, and the accompanying localization of the electronic structure is a critical determinant of the polymer's electroactive properties.[12] In the more localized electronic structure, the charged migration between the strands can be thought of as redox (self-exchange) conduction. Although this localization may not affect the short-range metal−polymer interactions or the metal−metal interactions, it usually reduces the overall conductivity of the materials. There are few examples of the conjugated polymers containing ferrocene units where the ferrocene sections are linked to the polymer backbone through one of the cyclopentadiene rings (Cp).[13] The principle reason for this limitation is the relative

† Part of the Electrochemistry special issue.

* Corresponding author. E-mail: tswager@mit.edu.

(1) (a) Manners, I. *Synthetic Metal-Containing Polymers*; Wiley-VCH: Weinheim, Germany, 2004. (b) Kingsborough, R. P.; Swager, T. M. *Prog. Inorg. Chem.* **1999**, *48*, 123.

(2) (a) Zhu, S. S.; Swager, T. M. *Adv. Mater.* **1996**, *8*, 497. (b) Zhu, S. S.; Swager, T. M. *J. Am. Chem. Soc.* **1997,** *119*, 12568. (c) Kingsborough, R. P.; Swager, T. M. *Adv. Mater.* **1998**, *11*, 1100. (d) Kingsborough, R. P.; Swager, T. M. *J. Am. Chem. Soc.* **1999**, *121*, 8825. (e) Kingsborough, R. P.; Swager, T. M. *Chem. Mater.* **2000**, *12*, 872. (f) Kingsborough, R. P.; Swager, T. M. *Angew. Chem., Int. Ed.* **2000**, *39*, 2897. (g) Vigalok, A.; Zhu, Z.; Swager, T. M. *J. Am. Chem. Soc.* **2001**, *123*, 7917. (h) Vigalok, A.; Swager, T. M. *Adv. Mater.* **2002**, *14*, 368. (i) Shioya, T.; Swager, T. M. *Chem. Commun.* **2002**, 1364. (j) Kwan, P. H.; Swager, T. M. *Chem. Commun.* **2005**, 5211.

(3) (a) Atwood, J. D. *Inorganic and Organometallic Reaction Mechanisms*; Wiley: New York, 1997. (b) Rodgers, G. E. *Introduction to Coordination, Solid State, and Descriptive Inorganic Chemistry*; McGraw-Hill: New York, 1994.

(4) Holliday, B. J.; Swager, T. M. *Chem. Commun.* **2005**, 23.

(5) Wolf, M. O. *Adv. Mater.* **2001**, *13*, 545.

(6) (a) Pickup, P. G. *J. Mater. Chem.* **1999**, *9*, 1641. (b) Cameron, C. G.; Pittman, T. J.; Pickup, P. G. *J. Phys. Chem. B* **2001**, *105*, 8838.

(7) Zotti, G.; Zecchin, S.; Schiavon, G.; Berlin, A.; Pagani, G.; Canavesi, A. *Chem. Mater.* **1995**, *7*, 2309.

(8) Martin, R. E.; Diederich, F. *Angew. Chem., Int. Ed.* **1999**, *38*, 1350.

(9) Cornil, J.; Beljonne, D.; Calbert, J.-P.; Brédas, J.-L. *Adv. Mater.* **2001**, *13*, 1053.

(10) (a) Altmann, M.; Enkelmann, V.; Beer, F.; Bunz, U. H. F. *Angew. Chem., Int. Ed. Engl.* **1995**, *34*, 569. (b) Tomita, I.; Nishio, A.; Endo, T. *Macromolecules* **1995**, *28*, 3042. (c) Bunz, U. H. F. *Pure Appl. Chem.* **1996**, *68*, 309. (d) Morisaki, Y.; Chen, H.; Chujo, Y. *Polym. Bull.* **2002**, *48*, 243.

(11) (a) Wolf, M. O.; Zhu, Y. *Adv. Mater.* **2000**, *12*, 599. (b) Higgins, S. J.; Jones, C. L.; Francis, S. M. *Synth. Met.* **1999**, *98*, 211. (c) Foucher, D. A.; Tang, B.; Manners, I. *J. Am. Chem. Soc.* **1992**, *114*, 6246. (d) Bureteau, M. A.; Tilly, T. D. *Organometallics* **1997,** *13*, 4367.

(12) Zhu, Y.; Wolf, M. O. *Chem. Mater.* **1999**, *11*, 2995.

10.1021/la061078h CCC: $33.50
Published on Web 08/16/2006

Scheme 1

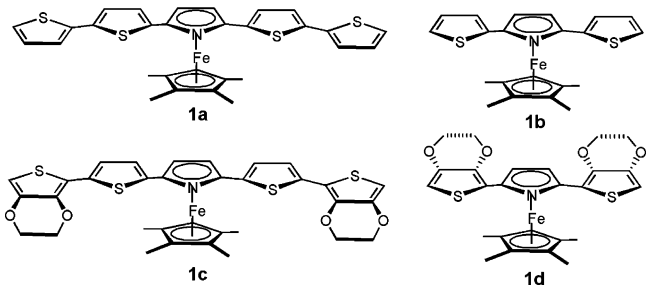

synthetic difficulty in attaching multiple groups to only one Cp ring of a ferrocene.[14]

Azaferrocene is isoelectronic with ferrocene and involves the substitution of one of the Cp rings of ferrocene with a pyrrolide ligand.[15] The reactivity of the parent pyrrole provides easy access to azaferrocene derivatives with thiophene substituents on the α positions, as shown in Scheme 1.[16] The polymerization of the azaferrocene derivatives through the coupling of the terminal thiophenes provides a fully conjugated polymer with a metal bound to the polymer backbone in a π fashion.

Azaferrocenes have not been widely investigated as an element in conducting polymers. The only previously investigated poly(azaferrocene) was produced by an innovative precursor approach wherein a $CpFe(CO)_2$ was first η^1 coordinated to an imine nitrogen within a polypyrrole.[17] Decarbonylation resulted in a reorganization to give the η^5-azaferrocene-containing polypyrrole. In our present study, we begin with azaferrocene that can be polymerized through attached thiophenes to give an azaferrocene−polythiophene hybrid material.

Even without a structural segmentation of the carbon-based π system, electronic localization can occur. The binding of the metal to the conducting polymer strand can induce localization of the π electrons of the polymer. This localization is caused by the binding of a metal to a monomer unit of the polymer, which can localize the molecular orbitals by effectively stabilizing (lowering the energy) the interacting π electrons of the monomer. This feature, which we term energetic localization, was studied by Mann and co-workers in their examination of ruthenium and osmium oligothiophene complexes and the oxidation potential of the organic fragment.[18] Our hypothesis is that although similar energetic localization may occur by the binding of the metal, this effect would not be as significant as that caused by the direct physical disruption of the π conjugation as in the case of 1,1′-substituted ferrocenes.

Maximized polymer-to-metal interactions are an important element in the design of efficient metal-to-organic conducting polymers. However, we also seek to maximize the metal−metal interactions to create materials with the optimal bulk electronic/magnetic properties. Plenio and co-workers investigated ferroceneacetylene-based oligomers and polymers, and the results suggested that the 1,3 substitution on the ferrocene provided strong metal−metal electronic interactions.[13] In describing the metal−metal interactions observed in conducting metallopolymers, Pickup and co-workers have made a useful distinction between the types of interactions that can exist between the metal centers. These interactions were described as superexchange interactions, direct charge hopping (similar to outer sphere inorganic electron transfer), and mediated charge transfer. For the superexchange interaction, classical studies on mixed-valance metal complexes provide a useful model for the description of these interactions.[19] In these mixed-valance complexes, the relative strength of the interaction between the metal centers can be described by a comproportionation constant, K_{com}. Most often K_{com} increases with a decrease in the length of a conjugated linker.[20] This increased interaction should affect the electroactivity of the polymer and may perhaps increase in the superexchange conduction process. To explore this idea, the length of the thiophene linkage (the conjugated linker) was systematically varied to study the effect of the metal−metal interaction on the electroactivity and conductivity of the resulting polymer.

The electronic transport (conductivity) will be dependent on the metal−polymer electron exchange and rates. We have previously utilized redox matching, wherein the oxidation potentials of the metal and the polymer are matched as closely as possible, to enhance these rates and consequently the electroactivity and conductivity.[2b,c] Pickup and co-workers have investigated the role of superexchange and used several different methods to interrogate conducting metallopolymers.[21] Their research focused on conducting polymers in which the organic elements were not electroactive over the potential ranges exhibited by the metal-centered redox couples. Hence, the role of the superexchange conduction mechanism on a conducting metallopolymer containing electroactive redox matched organic segments and metal centers remains an important question. The competitive, cooperative, or independent nature of the metal−metal interactions and how this influences the bulk conductive properties of a material must also be understood for the applications of these materials. Hence, both the length and the oxidation potential of the conjugated linkers between the azaferrocene units were varied to observe how both the mediated and superexchange mechanisms affect the overall polymer electroactivity.

We describe herein the synthesis and characterization of a series of polythiophene derivatives containing azaferrcoene that give polymers **p-1a**, **p-1b**, **p-1c**, and **p-1d** with a fully π-conjugated backbone as shown in Scheme 2. The monomers were anodically polymerized, and the resulting polymers were characterized by using cyclic voltammetry (CV), in situ conductivity, and spectroelectrochemistry. Our results suggest that the superexchange mechanism alters the electroactivity of these systems.

Experimental Section

General Comments. ^1H and ^{13}C NMR spectra were recorded on a Bruker 400 MHz spectrometer and are referenced to residual $CHDCl_2$ (5.32 ppm for ^1H and 54.00 ppm for ^{13}C). Melting points are uncorrected. High-resolution mass spectra (HRMS) were determined with a Bruker Daltonics APEX II 3 Tesla FT-ICR−MS. 2-Tributylstannyl-3,4-ethylenedioxythiophene, 5-tributylstannyl-[2,2′] bithiophene and 2,5-dibromo-1-(carboxylic acid *tert*-butyl ester)-pyrrole were synthesized according to published procedures.[2b,16] All commercial chemicals were purchased from Aldrich. Solvents were dried by passing through activated alumina and deoxygenated by purging with Ar or purified by an SPS-400-5 solvent purification system (Innovative Technologies). Air-sensitive manipulations were

(13) Plenio, H.; Hermann, J.; Sehring, A. *Chem.−Eur. J.* **2000**, *6*, 1820.
(14) Plenio, H.; Hermann, J.; Leukel, J. *Eur. J. Inorg. Chem.* **1998**, 2063.
(15) (a) Joshi, K. K.; Pauson, P. L.; Quazi, A. R.; Stubbs, W. H. *J. Organomet. Chem*. **1964**, *1*, 471. (b) King, R. B.; Bisnette, M. B. *Inorg. Chem.* **1964**, *3*, 796.
(16) Groenendaal, L.; Peerlings, H. W. I.; van Dongen, J. L. J.; Havinga, E. E.; Vekemans, J. A. J. M.; Meijer, E. W. *Macromolecules* **1995**, *28*, 116.
(17) Martin, K. F.; Hanks, T. W. *Organometallics* **1997**, *16*, 4857.
(18) Graf, D. D.; Mann, K. R. *Inorg. Chem*. **1997**, *36*, 150.
(19) (a) Robin, M. B.; Day, P. *Adv. Inorg. Chem. Radiochem.* **1967**, *10*, 247. (b) Allen, G. C.; Hush, N S. *Prog. Inorg. Chem.* **1967**, *8*, 357. (c) Demadis, K. D.; Hartshorn, C. M.; Meyer, T. J. *Chem. Rev.* **2001**, *101*, 2655.
(20) Barlow, S.; O'Hare, D. *Chem. Rev.* **1997**, *97*, 637.
(21) (a) Cameron, C. G.; Pickup, P. G. *Chem. Commun.* **1997**, 303. (b) Cameron, C. G.; Pickup, P. G. *J. Am. Chem. Soc.* **1999**, *121*, 7710. (c) Cameron, C. G.; Pickup, P. G. *J. Am. Chem. Soc.* **1999**, *121*, 11773.

Scheme 2. Oxidative Polymerization of 1a and Polymer Structures

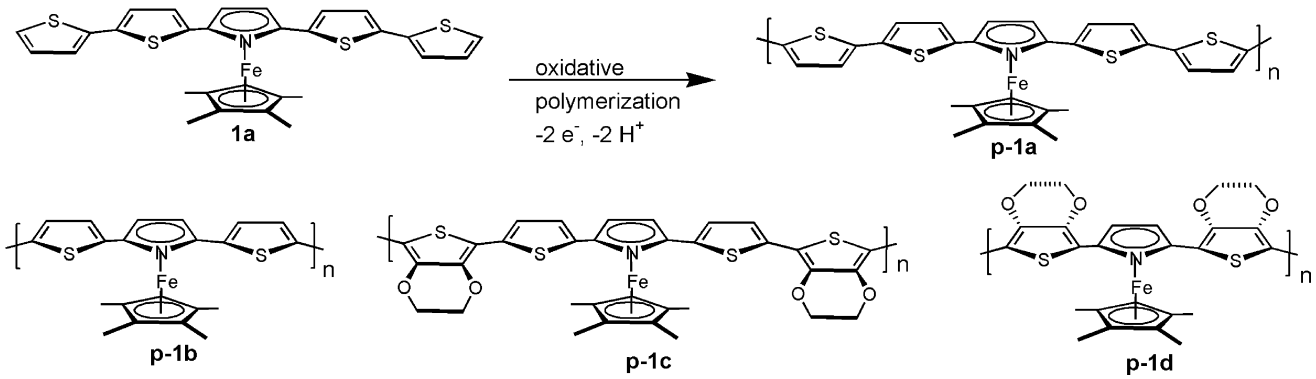

performed using standard Schlenk techniques. Electrochemical measurements were performed in a nitrogen glovebox with an Autolab II with a PGSTAT 30 potentiostat (Eco Chemie). The electrolyte solution for all electrochemical measurements, 0.1 M (n-Bu)$_4$NPF$_6$ in dry CH_2Cl_2, was stored over 4 Å molecular sieves in a glovebox. The quasi-internal reference electrode was a Ag wire submersed in 0.01 M $AgNO_3$/0.1 M (n-Bu)$_4$NPF$_6$ in anhydrous acetonitrile, and a Pt wire or gauze was used as a counter electrode. All potentials were referenced to the Fc/Fc$^+$ couple. The working electrodes were 5 or 10 μm Pt interdigitated microelectrodes (Abtech Scientific, Inc.) or indium tin oxide-coated unpolished float glass slides (Delta Technologies). Absorption spectra were collected on an Agilent 8453 diode array spectrophotometer or a Carey 6000i UV−vis−NIR spectrophotometer. A Dektak 6M stylus profiler (Veeco) was used to measure the film thickness of the polymers grown onto interdigitated microelectrodes. X-ray photoelectron spectroscopy measurements were collected on a Kratos Axis Ultra Imaging X-ray photoelectron spectrometer.

2,5-Bis-(5-[2,2′]-bithiophene)-1-(carboxylic acid *tert*-butyl ester)-pyrrole (2a). In a 100 mL Schlenk tube, 0.267 g of 2,5-dibromo-1-(carboxylic acid *tert*-butyl ester)-pyrrole, 2.0 g of 5-tributylstannyl-[2,2′] bithiophene, 2.2 g of KF, and 50 mL of toluene were combined. The solution was deoxygenated by purging with Ar for 30 min. To the solution was added 0.078 g of Pd_2dba_3 and 0.048 g of HP(*tert*-Bu)$_3$BF$_4$, and the solution was stirred for 48 h. Water was added, and the product was isolated by extraction with CH_2Cl_2. The organic layer was dried with $MgSO_4$, and the solvent was evaporated in vacuo. Column chromatography was performed with silica gel (the silica gel was pretreated with 10% triethylamine in hexanes before the column was run) using 28% CH_2Cl_2 in hexanes as an eluent. After evaporation of the solvent under reduced pressure, 0.173 g (42%) of the product was obtained as a bright-yellow solid, mp 127.2 °C. ^{1}H NMR (CD_2Cl_2): δ 7.30 (dd J = 3.6, 1.1 Hz, 2 H), 7.27 (dd J = 4.7, 1.1 Hz, 2 H), 7.20 (d J = 3.7 Hz, 2 H), 7.10 (dd J = 4.7, 3.6 Hz, 2 H), 7.07 (d J = 3.7 Hz, 2 H), 6.44 (s, 2 H), 1.42 (s, 9 H). ^{13}C NMR (CD_2Cl_2): δ 149.8, 137.7, 137.5, 133.7, 129.2, 128.4, 128.1, 125.0, 124.2, 123.9, 114.2, 85.5, 27.5. HRMS Calcd for $C_{25}H_{21}NO_2S_4$ [M]$^+$: 495.0450. Found: 495.0470.

2,5-Bis-(5-[2,2′]-bithiophene)-1′,2′,3′,4′,5′-pentamethylazaferrocene (1a). In a glovebox, 0.116 g of **2a**, 0.20 g of sodium methoxide, and 5 mL of THF were stirred together for 3 h. During that time in a separate flask, 0.037 g of 1,2,3,4,5-pentamethyl cyclopentadiene (Cp*H) and 0.35 mL of a 2.2 M solution of n-BuLi were stirred together in 5 mL of THF for 1.5 h. Subsequently, 0.094 g of $FeCl_2$ was added to the Cp*Li solution and stirred an additional 1.5 h. The mixtures of **2a** and Cp*FeCl were added together and stirred for 16 h. After stirring, the solution was taken out of the glovebox and filtered through a column of silica gel using ethyl acetate as an eluent. The solvent was removed in vacuo. Column chromatography was performed with silica gel (the silica gel was pretreated with 10% triethylamine in hexanes before the column was run) using a solution of 10% ethyl acetate in hexanes as an eluent. After evaporation of the solvent under reduced pressure, 0.071 g (53%) of the product was obtained as an orange solid, mp 147 °C. The product was stored in a glovebox. ^{1}H NMR (CD_2Cl_2): δ 7.30 (broad m; apparent s, 4 H), 7.19 (broad m; apparent d, 4 H), 7.08 (apparent s, 2 H) 4.66 (s, 2 H), 1.58 (s, 15 H). ^{13}C NMR (CD_2Cl_2): δ 139.2, 138.4, 135.9, 128.5, 124.7, 124.4, 123.7, 123.6, 99.4, 82.6, 72.4, 9.4. HRMS Calcd for $C_{30}H_{28}FeNS_4$ [M + H]$^+$: 586.0459. Found: 586.0480.

2,5-Bis-[2-thiophene]-1-(carboxylic acid *tert*-butyl ester)-pyrrole (2b). In a 50 mL Schlenk flask, 0.297 g of 2,5-dibromo-1-(carboxylic acid *tert*-butyl ester)-pyrrole, 1.4 g of 2-tributylstannylthiophene, 1.7 g of KF, and 20 mL of toluene were combined. The solution was deoxygenated by purging with Ar for 30 min. To the solution was added 0.080 g of Pd_2dba_3 and 0.040 g of HP(*tert*-Bu)$_3$BF$_4$, and the solution was then stirred for 40 h. Water was added, and the product was isolated by extraction with ethyl acetate. The organic layer was dried with $MgSO_4$, and the solvent was evaporated in vacuo. The isolated product was purified by column chromatography with silica gel (the silica gel was pretreated with 10% triethylamine in hexanes before the column was run to avoid oxidation) using 10% CH_2Cl_2 in hexanes as an eluent. After removal of the solvent by evaporation, the product was obtained as a slightly yellow solid, 0.149 g (49%), mp 90 °C. ^{1}H NMR (CD_2Cl_2): δ 7.39 (dd J = 5. 0, 1.4 Hz, 2 H), 7.11 (m, 4 H), 6.37 (s, 2 H), 1.31 (s, 9 H). ^{13}C NMR (CD_2Cl_2): δ 149.9, 134.9, 129.2, 127.6, 127.4, 126.1, 114.0, 85.2, 27.5. HRMS Calcd for $C_{17}H_{17}NO_2S_2$ [M]$^+$: 331.0695. Found: 331.0696.

2,5-Bis-(2-thiophene)-1′,2′,3′,4′,5′-pentamethylazaferrocene (1b). In a glovebox, 0.090 g of **2b**, 0.12 g of sodium methoxide, and 5 mL of THF were stirred together for 3 h. During that time in a separate flask, 0.025 g of Cp*H and 0.12 mL of a 2.2 M solution of n-BuLi were stirred together in 5 mL of THF for 1.5 h. Subsequently, 0.035 g of $FeCl_2$ was added to the Cp*Li solution, which was stirred an additional 1.5 h. The mixtures of **2b** and Cp*FeCl were added together and stirred at room temperature for 28 h. The solution was then taken out of the glovebox and filtered through a column of silica gel using ethyl acetate as an eluent, and the solvent was then removed in vacuo. Column chromatography was performed with silica gel (the silica gel was pretreated with 10% triethylamine in hexanes before the column was run) using a mixture of 10% ethyl acetate in hexanes as an eluent. After evaporation of the solvent under reduced pressure, 0.041 g (36%) of the product was obtained as an orange solid, mp 133.3 °C. The product was stored in a glovebox. ^{1}H NMR (CD_2Cl_2): δ 7.30 (broad m, 4 H), 7.12 (apparent broad triplet, 2 H), 4.64 (s, 2 H), 1.52 (s, 15 H). ^{13}C NMR (CD_2Cl_2): δ 140.1, 128.1, 124.0, 123.1, 99.6, 82.3, 72.2, 9.3. HRMS Calcd for $C_{22}H_{23}FeNS_2Na$ [M + Na]$^+$: 444.05190. Found: 444.0528.

2,5-Bis-[5-bromo-2-thiophene]-1-(carboxylic acid *tert*-butyl ester)-pyrrole (3). In a 100 mL round-bottomed flask, we placed 0.146 g of **2b**, which then dissolved in 25 mL of dimethylformamide. To this solution was added 0.165 g of *N*-bromosuccimide dissolved in 25 mL of dimethylformamide. The solution was stirred for 12 h. Water was added to the mixture, and the product was extracted with ethyl ether. The organic layer was dried with $MgSO_4$, and the solvent was removed in vacuo. Column chromatography was performed with a short column of silica gel using hexanes as an eluent. After evaporation of the solvent under reduced pressure, 0.178 g (83%) of the product was obtained as a slightly yellow solid, mp 91 °C.

^{1}H NMR (CD_2Cl_2): δ 7.05 (d J = 3.8 Hz, 2 H), 6.87 (d J = 3.8 Hz, 4 H), 6.35 (s, 2 H), 1.34 (s, 9 H). ^{13}C NMR (CD_2Cl_2): δ 149.4, 136.6, 130.2, 128.7, 128.3, 114.9, 112.6, 85.7, 27.6. HRMS Calcd for $C_{17}H_{15}Br_2NO_2S_2$ $[M]^+$: 486.8905. Found: 486.8922.

2,5-Bis-(5-(2-[3,4-ethylenedioxythiophene]thiophene)-1-(carboxylic acid *tert*-butyl ester)-pyrrole (2c). In a 50 mL Schlenk flask, 0.178 g of 2,5-bis-[5-bromo-2-thiophene]-1-(carboxylic acid *tert*-butyl ester)-pyrrole, 1.0 g of 2-tributylstannyl-3,4-ethylenedioxythiophene, 1.4 g of KF, and 20 mL of toluene were combined. The solution was deoxygenated by purging with Ar for 30 min. To the solution was added 0.080 g of Pd_2dba_3 and 0.040 g of HP(*tert*-Bu)$_3BF_4$, and the solution was then stirred for 20 h. Water was added, and the product was isolated by extraction with ethyl acetate. The organic layer was dried with $MgSO_4$, and the solvent was evaporated in vacuo. Column chromatography with silica gel (the silica gel was pretreated with 10% triethylamine in hexanes before the column was run) was performed using a gradient of 20 to 40% ethyl acetate in hexanes as an eluent. After evaporation of the solvent under reduced pressure, 0.145 g (65%) of the product was obtained as a yellow solid, mp 169 °C (dec). ^{1}H NMR (CD_2Cl_2): δ 7.19 (d J = 3.8 Hz, 2 H), 7.03 (broad d with an apparent J = 3.3 Hz, 2 H), 6.40 (s, 2 H), 6.28 (s, 2 H), 4.37 (m, 4 H), 4.28 (m, 4 H), 1.39 (s, 9 H). ^{13}C NMR (CD_2Cl_2): δ 150.1, 142.6, 138.3, 135.3, 132.9, 129.4, 127.3, 123.0, 113.9, 112.2, 97.4, 85.6, 65.6, 65.2, 27.6. HRMS Calcd for $C_{29}H_{25}NO_6S_4Na$ $[M + Na]^+$: 634.0457. Found, 634.0441.

2,5-Bis-(5-(2-[3,4-ethylenedioxythiophene]thiophene)-1′,2′,3′,4′,5′-pentamethylazaferrocene (1c). In a glovebox, 0.108 g of **2c**, 0.20 g of sodium methoxide, and 5 mL of THF were stirred together for 3.5 h. During that time, 0.028 g of Cp*H and 0.1 mL of a 2.2 M solution of *n*-BuLi were stirred together in 5 mL of THF for 1.5 h. Subsequently, 0.035 g of $FeCl_2$ was added to the Cp*Li solution, which was stirred an additional 1.5 h. The mixtures of **2c** and Cp*FeCl were added together and then stirred for an additional 20 h. After stirring, the solution was taken out of the glovebox and filtered through a column of silica gel using ethyl acetate as an eluent. The solvent was removed in vacuo. Column chromatography was performed using silica gel (the silica gel was treated with 10% triethylamine in hexanes before the column was run) and a mixture of 30% ethyl acetate in hexanes as an eluent. After evaporation of the solvent under reduced pressure, 0.034 g (27%) of the product was obtained as an orange solid, mp 254 °C (dec). The product was stored in a glovebox. ^{1}H NMR (CD_2Cl_2): δ 7.24 (broad d J = 3.6 Hz, 2 H), 7.19 (broad d J = 3.6 Hz, 2 H) 6.27 (s, 2 H), 4.65 (s, 2 H), 4.41 (m, 4 H), 4.32 (m, 4 H), 1.58 (s, 15 H). ^{13}C NMR (CD_2Cl_2): δ 142.7, 138.3, 137.9, 133.6, 123.7, 123.2, 113.1, 99.7, 96.7, 82.5, 72.2, 65.7, 65.3, 9.5. HRMS Calcd for $C_{26}H_{28}FeNO_4S_2$ $[M + H]^+$: 702.0569. Found: 702.0575.

2,5-Bis-(2-[3,4-ethylenedioxythiophene])-1-(carboxylic acid *tert*-butyl ester)-pyrrole (2d). In a 50 mL Schlenk flask, 0.343 g of 2,5-dibromo-1-(carboxylic acid *tert*-butyl ester)-pyrrole, 1.0 g of 2-tributylstannyl-3,4-ethylenedixoythiophene, 0.30 g of KF, and 20 mL of toluene were combined. The solution was deoxygenated by purging with Ar for 30 min. To the solution was added 0.048 g of Pd_2dba_3 and 0.020 g of HP(*tert*-Bu)$_3BF_4$, and the solution was then stirred for 48 h. Water was then added, and the product was extracted with CH_2Cl_2. The organic layer was dried with $MgSO_4$, and the solvent was removed in vacuo. Column chromatography was performed with silica gel (the silica gel was pretreated with 10% triethylamine in hexanes before the column was run) using 20% ethyl acetate in hexanes as an eluent. After evaporation of the solvent under reduced pressure, 0.262 g (55%) of the product was obtained as a slightly yellow solid, 155−158 °C (dec).^{1}H NMR (CD_2Cl_2): δ 6.38 (s, 2 H), 6.26 (s, 2 H), 4.22 (s, 8 H), 1.38 (s, 9 H). ^{13}C NMR (CD_2Cl_2): δ 149.2, 141.6, 139.3, 125.9, 114.6, 108.9, 98.8, 83.9, 65.2, 65.0, 27.5. HRMS Calcd for $C_{21}H_{21}NO_6S_2Na$ $[M + Na]^+$: 470.0702. Found: 470.0702.

2,5-Bis-(3,4-ethylenedioxythiophene)-1′,2′,3′,4′,5′-pentamethylazaferrocene (1d). In a glovebox, 0.194 g of **2d**, 0.30 g of sodium methoxide, and 5 mL of THF were stirred together for 3 h. During that time in a separate flask, 0.085 g of Cp*H and 0.35 mL of a 2.2 M solution of *n*-BuLi were stirred together in 5 mL of THF for 1.5 h. Subsequently, 0.085 g of $FeCl_2$ was added to the Cp*Li solution, which was stirred an additional 1.5 h. The mixtures of **2d** and Cp*FeCl were added together and stirred for 28 h. After stirring, the solution was taken out of the glovebox and filtered through a short column of silica gel using ethyl acetate as an eluent, and the solvent was then removed in vacuo. Column chromatography was performed with silica gel (the silica gel was pretreated with 10% triethylamine in hexanes before the column was run) using a mixture of 1:1 ethyl acetate and hexanes as an eluent. After evaporation of the solvent under reduced pressure, 0.117 g (50%) of the product was obtained as an orange solid, 250° (dec) C. The product was stored in a glovebox. ^{1}H NMR (CD_2Cl_2): δ 6.28 (s, 2 H), 4.86 (s, 2 H), 4.40 (m, 4 H), 4.29 (m, 4 H), 1.58 (s, 15 H). ^{13}C NMR (CD_2Cl_2): δ 142.5, 138.2, 114.0, 97.3, 97.1, 81.8, 73.3, 65.4, 65.3, 9.3. HRMS Calcd for $C_{26}H_{28}FeNO_4S_2$ $[M + H]^+$: 538.0814. Found: 538.0805.

Results and Discussion

Synthesis. The starting pyrrole compounds needed for the target azaferrocenes were synthesized by Stille cross-coupling reactions of the appropriate thiophene units with 2,5-dibromo-1-(carboxylic acid *tert*-butyl ester)-pyrrole, as shown in Scheme 3.[16,22] The BOC groups in **2a**−**d** were removed by treatment with sodium methoxide in THF, and the deprotected pyrroles were then reacted in situ with the half sandwich complex of Cp*FeCl to produce the appropriate azaferrocenes. The molecular structure of **1a** was confirmed by single-crystal X-ray diffraction.

Monomers **1a**−**d** were subjected to anodic polymerization conditions in an electrolyte solution of 0.1 M (n-Bu)$_4$NPF$_6$ in CH_2Cl_2 to give polymers **p-1a**, **p-1b**, **p-1c**, and **p-1d** as shown in Scheme 2.[23] As shown in Figure 1, for this polymerization, the potential was cycled between a potential where a chemically irreversible oxidation (polymerization) occurred and then back to a potential wherein the material is fully reduced. The azaferrocene electrochemistry is prominent in the first cycle but is subsequently overlapped by the large electroactivity of the conducting polymer that deposits on the electrode with each cycle. The observed reversible $Fe^{II/III}$ redox potential is in accord with previous electrochemical work on azaferrocene complexes.[24] A summary of the results is listed in Table 1.

Energetic Localization versus Structural Localization. As mentioned earlier, we are interested in assessing the effect of energetic versus structural localization on the polymer's electroactivity and conductivity. In **p-1a**, the oxidation potential of the organic fragments is higher than the metal-centered electroactivity. The azaferrocene units are separated by relatively long conjugated linkers that contain four thiophene units. Both of these effects should decrease the interaction between the individual metal centers of the polymer. The cyclic voltammetry (CV) of **p-1a** displays two waves with half-wave potentials ($E_{1/2}$'s) near approximately 0.10 and 0.49 V, as shown in Figure 2. An analysis of the atomic composition of **p-1a** by X-ray photoelectron spectroscopy gave a ratio of 4.28:1 S/Fe for the atomic composition of the polymer.

The wave at 0.1 V was assigned to the $Fe^{II/III}$ redox couple of the complex because it was closest in potential to the wave assigned as the $Fe^{II/III}$ redox couple in the initial CV scan of the monomer. The $E_{1/2}$ of the second wave in the CV of **p-1a** was

(22) Netherton, M. R.; Fu, G. C. *Org. Lett.* **2001**, *3*, 4295.

(23) The polymerizations reported here create insoluble coatings on the electrode surface, and hence molecular weight and regiochemical determinations of these polymers cannot be determined. However, related anodic polymerizations of soluble thiophenes typically display a regiochemical preference of >95% for creating thiophene couplings between carbons alpha to the sulfur centers. The degree of polymerization for soluble polythiophenes (e.g., 3-alkylthiophenes) polymerized electrochemically ranges from 300 to 90 (Roncali, J. *Chem. Rev.* **1992**, *92*, 711).

(24) (a) Audebert, P.; Miomandre, F.; Zakrzewski, J. *J. Electroanal. Chem.* **2002**, *530*, 63. (b) Nakashima, S.; Tanaka, M.; Okuda, T. *Inorg. Chem. Commun.* **2002**, *5*, 312.

Scheme 3. Synthesis of the Azaferrocene Complexes

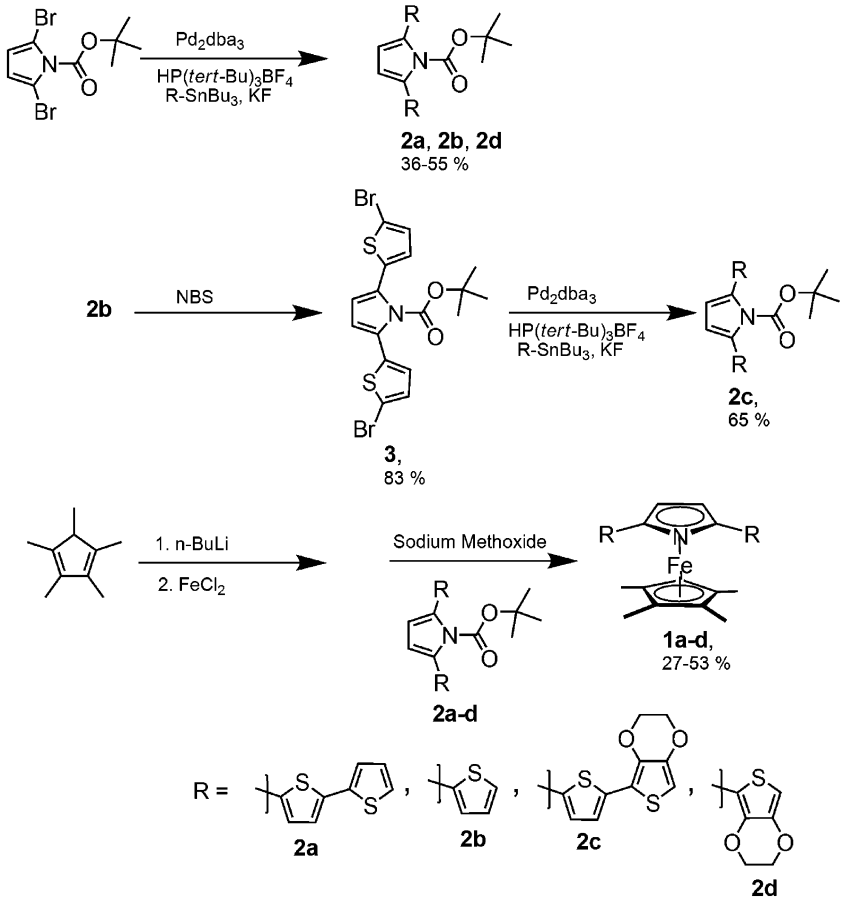

similar to previously reported $E_{1/2}$'s for quarterthiophenes oligomers, so this wave was categorized as the oxidation of the quarterthiophene section of the polymer.[25] This categorization was also based on the idea that the binding of Fe to the pyrrole

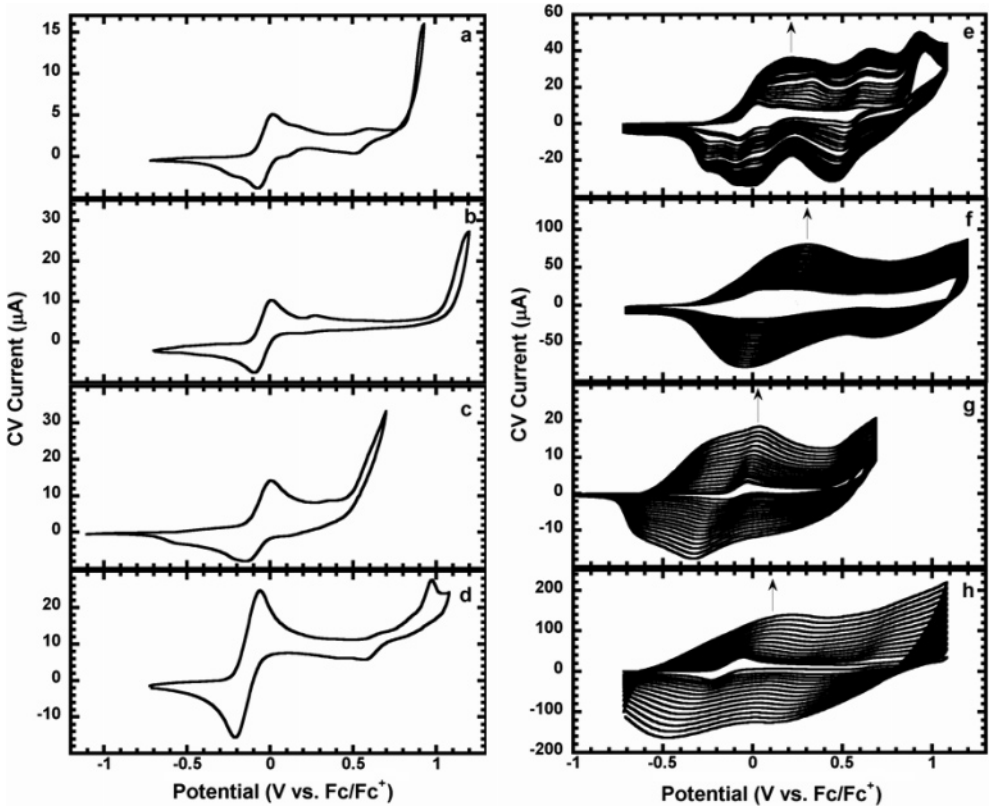

Figure 1. Initial cyclic voltammogram scans and polymerizations of complexes **1a** (**a** and **e**), **1b** (**b** and **f**), **1c** (**c** and **g**), and **1d** (**d** and **h**) at 100 mV/s in 0.1 M $(n\text{-Bu})_4NPF_6$ in CH_2Cl_2 with an interdigitated 5 μm Pt microelectrode as the working electrode.

Table 1. Electrochemical and UV−Vis Data of Complexes 1a−d and Corresponding Polymers

complex	monomer[a] $E_{1/2}$ (V)	monomer[a] E_{pa} (V)	monomer[b] λ_{max} (nm)	polymer[c] E_{pa} (V)	polymer[d] λ_{max} (nm)	σ_{max} (S cm^{-1})
1a	−0.0	0.02	360, 431 (sh)	0.17	435	0.0047
1b	−0.04	0.02	296, 391 (sh)	0.33	463	0.0052
1c	−0.07	0.00	366, 435 (sh)	0.00	572, 586	0.0092
1d	−0.14	−0.07	301 393 (sh)	−0.02	503, 537, 592	0.0095

[a] The values refer to the first wave in the CV of the monomer. [b] The UV−vis spectra were obtained in CH_2Cl_2 (sh = shoulder). [c] The values refer to the first wave of the CV of the polymer. [d] These values are for the neutral (undoped) polymer.

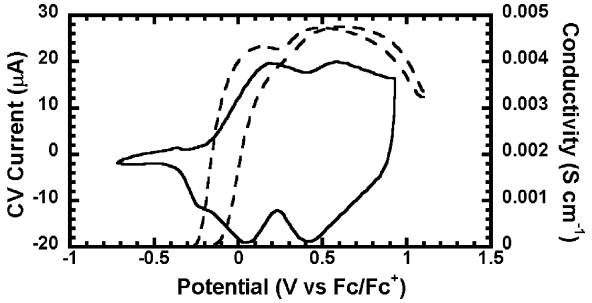

Figure 2. Cyclic voltammogram (solid line) at 100 mV/s and in situ conductivity (dashed line) of **p-1a** grown onto interdigitated 5 μm Pt microelectrodes at 10 mV/s with a 40 mV offset potential between the working electrodes.

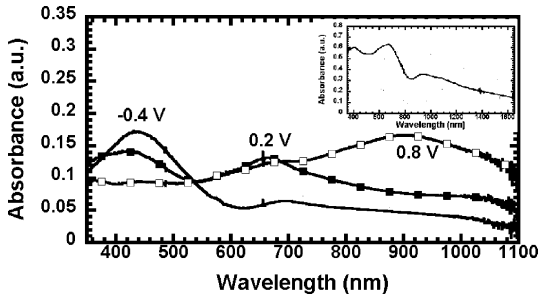

Figure 3. UV−vis absorption of a film of **p-1a** on ITO at potentials of the electrochemical cell set at −0.4 (−), 0.2 (■), and 0.8 V (□). The inset is the UV−vis/near-IR absorption of a film of **p-1c** with the potential of the electrochemical cell set at 0.2 V.

unit would produce a break in the π-conjugation from pyrrole to the thiophenes, which is consistent with Mann's previous findings.[18] The CV of **p-1a** suggested that the polymer should have the conductive properties of a charge-localized polymer, and the in situ conductivity of **p-1a** was to some extent consistent with this idea. The conductivity of **p-1a** in the in situ conductivity experiment of **p-1a**, shown in Figure 2, increased significantly at potentials near the metal oxidation and then continued to increase until the potential of the electrochemical cell approached the oxidation of the quarterthiophene fragment.[26] After that point, the conductivity went down. The confinement of the region of high conductivity to potential windows corresponding to the waves in the CV is consistent with a charge-localized polymer. Charge-localized polymers typically have much smaller areas of conductivity that are strictly confined to the potentials corresponding to the waves of the polymer CV.[27] Fully extended π-conjugated polymers with a significant amount of charge delocalization have much larger windows of conductivity, and these windows typically extend well beyond the potentials of the initial waves of the polymer CV.[28] This result is consistent with the idea of energetic localization of the polymer.

A spectroelectrochemistry study of **p-1a**, shown in Figure 3, was performed to provide more information about the polymer's response to oxidation. In agreement with the in situ conductivity, a change in the potential of the electrochemical cell from a potential where the polymer is neutral[29] (−0.4 V, λ_{max} = 435 nm) to a potential near the $Fe^{II/III}$ redox couple (0.2 V) produces a new peak in the absorbance, λ_{max} = 662 nm, of the film absorption. Upon oxidation at a potential near the quarterthiophene fragment oxidation (0.8 V), a red shift to a broad absorption emerges with a prominent feature centered at 900 nm in the absorbance of **p-1a**. The spectroelectrochemistry of an analogous polymer based on a 1,1′-bithiophene-substituted ferrocene, **p-2**, provides an interesting comparison.[12] The neutral absorbance of **p-2** has a λ_{max} at 445 nm, and upon oxidation at potentials near the $Fe^{II/III}$ redox couple (0.8 V vs SCE), the λ_{max} shifted to 495 nm and a weaker band appeared at 1395 nm. The higher-energy absorbance at 495 nm was assigned as the $\pi \rightarrow \pi^*$ of the quarterthiophene section with some possible contributions from a Cp to Fe^{III} ligand-to-metal charge-transfer band. The shift in wavelength of the λ_{max}'s of the UV−vis spectrum of the polymer from the neutral state to the metal oxidized state was significantly different for **p-1a** (227 nm) than for **p-2** (50 nm). This result suggests that the fully π-conjugated backbone in **p-1a** promotes the delocalization of charge throughout the polymer and the structural localization of **p-2** is more significant than the energetic localization of **p-1a**. The lower-energy absorbance (1395 nm) was assigned as a charge-transfer band from the quaterthiophene section (LMCT band) to the Fe^{III}. A similar lower-energy absorbance was not observed in **p-1a**. The absorption spectrum of **p-1a**, as shown in the inset of Figure 3, when oxidized at a potential corresponding to the $Fe^{II/III}$ redox couple displays a very broad absorption in the relevant region. However, it was assumed that a distribution of LMCT bands may have contributed to this absorption in the near-IR region by **p-1a** in this oxidized state. Oxidation at a higher potential (1.5 V vs SCE) in **p-2**, which was assumed to be the oxidation of the quarterthiopene section, produced a UV−vis absorbance spectrum that had a broad absorption with a feature centered near 900 nm. This result is similar to the spectroelectrochemical results of **p-1a** when the quarterthiophene section of **p-1a** was oxidized and suggested that at this oxidized state **p-1a** and **p-2** had similar charge delocalizations.

Superexchange Mechanism. The comparison of **p-1b** to **p-1a** is useful in the study of how the superexchange mechanism affects the conductivity. As stated in the Introduction, the decrease in the length of the oxidizable thiophene linker between the Fe sites in **p-1b** (bithiophene linker) versus **p-1a** (quarterthiophene linker) should lead to an increase in the metal−metal interactions. There is precedent for the improvement of the K_{com} for binuclear metallocene complexes as the length of an aryl conjugated linker between the metallocene units is decreased.[30]

As in **p-1a**, the CV of **p-1b** displayed two waves. The $E_{1/2}$ of the first wave in **p-1b** was at approximately the same potential

(25) Guay, J.; Kasai, P.; Diaz, A.; Wu, R.; Tour, J. M.; Dao, L. H. *Chem. Mater*. **1992**, *4*, 1097.
(26) (a) Zotti, G.; Schiavon, G. *Synth. Met.* **1990,** *39*, 183. (b) Schiavon, G.; Sitran, S.; Zotti, G. *Synth. Met.* **1989**, *32*, 209.
(27) Yu, H.-h.; Xu, B.; Swager, T. M. *J. Am. Chem. Soc.* **2003**, *125*, 1142.
(28) (a) Ofer, D.; Wrighton, M. S. *J. Am. Chem. Soc.* **1988**, *110*, 4467. (b) Ofer, D.; Crooks, R. M.; Wrighton, M. S. *J. Am. Chem. Soc*. **1990**, *112*, 7869.

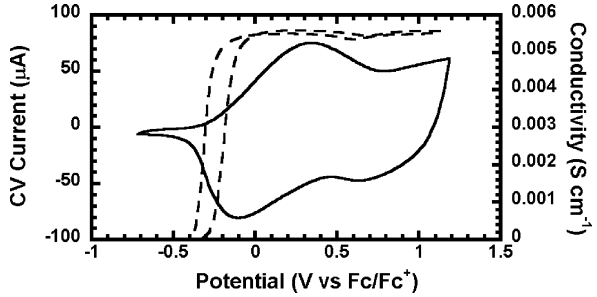

Figure 4. Cyclic voltammogram (−) at 100 mV/s and in situ conductivity (- -) of **p-1b**. The same in situ conductivity conditions for **p-1a** were used for **p-1b**.

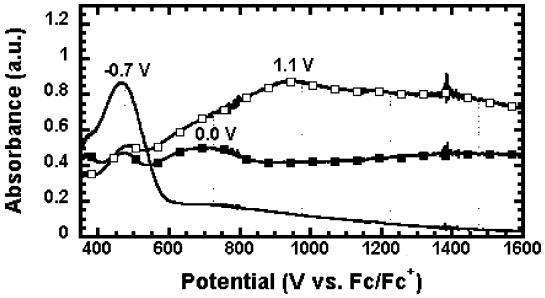

Figure 5. UV−vis absorption of a film of **p-1b** on ITO at potentials of the electrochemical cell set at −0.7 (−), 0.0 (■), and 1.1 V (□).

as the half-wave potential of the corresponding wave in **p-1a**. The exact point of the $E_{1/2}$ of the second wave of **p-1b** could not be precisely determined because the peak oxidation was beyond the edge of the solvent window. Hence, the $E_{1/2}$ for **p-1b**'s second wave, as shown in Figure 4, is at a significantly higher potential than the half-wave potential of the second wave of **p-1a**. Using the same logic as the wave assignment in **p-1a**, the first wave in the CV of **p-1b** was assigned to the $Fe^{II/III}$ redox couple, and the higher oxidation was considered to be the oxidation of the bithiophene section. For the $Fe^{II/III}$ redox couple, the separation between the peak oxidation potential and the peak reduction potential of **p-1b** (0.46 V) was significantly larger than the separation observed for **p-1c** (0.12 V). For a completely reversible surface-confined electrochemical event, the separation between the oxidation and reduction peaks of the CV wave should be zero.[31] However, conducting polymers often show significant peak separation in their CVs. This separation is generally attributed to poor electrochemical kinetics (limited charge and ion mobility) caused by a thick polymer film on the electrode.[32] However, the differences in the thicknesses of the polymer films were only about 20% (2000 Å for **p-1b** and 1600 Å for **p-1a**), so other causes for this disparity between the peak separation of the first wave in the CVs of **p-1b** and **p-1a** cannot be ruled out.

The in situ conductivity of **p-1b**, like that of **p-1a,** had an onset of conductivity that was coincident with the onset of oxidation of the $Fe^{II/III}$ redox couple wave, as shown in Figure 4. The onset of conductivity was lower in potential for **p-1b** than for **p-1a** and parallels the lower potential for the $Fe^{II/III}$ redox wave in **p-1b** as compared to that in **p-1a**. The in situ conductivity of **p-1b** had a significantly smaller hysteresis than that of **p-1a**. The lack of significant hysteresis in the in situ conductivity of **p-1b** can be attributed to a decrease in the structural changes of the polymer during the experiment.[33] The in situ conductivity of **p-1b** does display a small local minimum near the end of the $Fe^{II/III}$ redox wave. In contrast to **p-1a**, the in situ conductivity of **p-1b** does not show a decrease in conductivity at higher potentials. This outcome may be due to the fact that the organic oxidation wave is outside the potential window of the solvent (CH_2Cl_2).

The spectroelectrochemistry of **p-1b** displays interesting phenomena when compared to the spectroelectrochemistry of **p-1a**, as shown in Figure 5. The λ_{max} in the UV−vis spectrum of the neutral form of **p-1b** is 463 nm, which is a 28 nm bathochromic shift from the λ_{max} of **p-1a**. As in the spectroelectrochemistry of **p-1a**, the UV−vis absorption spectrum of **p-1b** changed significantly at potentials near the $Fe^{II/III}$ redox couple wave, and the UV−vis spectrum displayed a new λ_{max} at approximately 690 nm. The slight bathochromic shift of 28 nm in the neutral forms relative to the absorbance of **p-1a** is maintained with the oxidation of the metal sites in **p-1b**. Consistent with the differences in the onset of conductivities is that **p-1b** displayed this change in the UV−vis spectrum at a lower potential (0.0 V) than **p-1a**. With the oxidation of the Fe centers, the relative absorption of **p-1b** in the near-IR was more pronounced than that of **p-1a**. In the fully oxidized state, the dominant UV−vis absorbance at 930 nm of **p-1b** displays a slight red shift in comparison to analogous feature in the UV−vis spectrum of **p-1a**. In total, all of these spectroelectrochemical properties suggest improved delocalization in **p-1b** relative to that in **p-1a**.

Redox Matching. Redox matching involves the systematic modification of the organic polymer to make its redox potential commensurate with the metal-centered redox potential, and we have previously shown that this will improve both the electroactivity and conductivity of the polymer.[2c,34] Although the previously discussed azaferrocene polymers, **p-1a** and **p-1b**, display significant conductivity and electroactivity, we speculated that these properties could still be increased with redox matching. Given that the oxidation potentials of the organic fragments of these materials were higher than the $Fe^{II/III}$ redox couples, the oxidation potential of the organic fragments needed to be lowered to meet the matching condition. The substitution of a thiophene unit with a 3,4-ethylenedioxythiophene (EDOT) group was used to lower the oxidation potential of the organic section. An important issue is that the electron density donation from the electron-rich EDOT unit can also lower the potential of $Fe^{II/III}$ redox couple. The initial scans of **1c** and **1d**, as shown in Figure 1, display this effect with their $Fe^{II/III}$ redox couples occurring at lower potentials than the redox couples of **1a** and **1b**. However, this donation effect of the EDOT on the $Fe^{II/III}$ redox couple was smaller than the effect of the EDOT group on the oxidation potential of the organic fragment. In the end, the overall effect of the substitution of the EDOT groups is to bring the potential of the $Fe^{II/III}$ redox couple and the potential of the oxidation of the organic fragment closer to each other.

The effect of the addition of the EDOT groups is readily apparent in the CV of **p-1c**, as shown in Figure 6. The CV of **p-1c** had only one broad oxidation peak at −0.02 V and two unresolved reduction peaks at −0.31 and −0.66 V. This result is in stark contrast to its simple thiophene homologue **p-1a**, which had two clear oxidation waves. On the basis of comparisons with other polymers, the electroactivity around −0.02 V contained both the $Fe^{II/III}$ redox couple and thiophene-centered

(29) The UV−vis spectrum of the neutral polymer contained a long-wavelength absorbance tail that was assumed to be due to an incomplete reduction of the polymer film after the anodic polymerization.

(30) Bunel, E. E.; Campos, P.; Ruz, J.; Valle, L.; Chadwick, I.; Santa Ana, M.; Gonzalez, G.; Manriquez, J. M. *Organometallics* **1988**, *7*, 474.

(31) Bard, A. J.; Faulker, L. R. *Electrochemical Methods: Fundamentals and Applications*, 2nd ed.; Wiley & Sons: New York, 2001.

(32) *Handbook of Conducting Polymers*; Skotheim, T. A., Elsenbaumer, R. L., Reynolds, J. R., Eds.; Marcel Dekker: New York, 1998.

(33) Chung, T.-C.; Kaufman, J. H.; Heeger, A. J.; Wudl, F. *Phys. Rev. B* **1984**, *30*, 702.

(34) Zhu, Y.; Wolf, M. O. *J. Am. Chem. Soc.* **2000**, *122*, 10121.

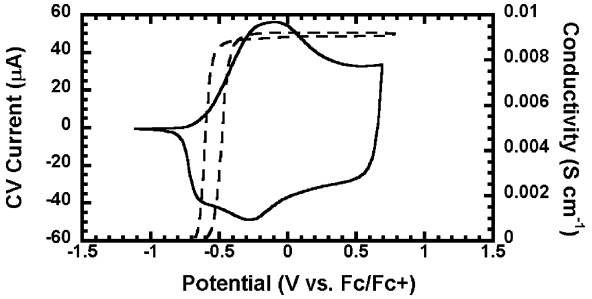

Figure 6. Cyclic voltammogram (−) at 100 mV/s and in situ conductivity (- -) of **p-1c** grown onto interdigitated 10 μm Pt microelectrodes at 10 mV/s with a 40 mV offset potential between the working electrodes.

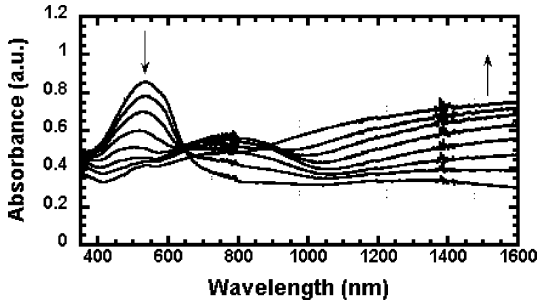

Figure 7. Spectroelectrochemistry of **p-1c** grown onto ITO with potential changes from −0.5 to 0.1 V in 0.1 V intervals.

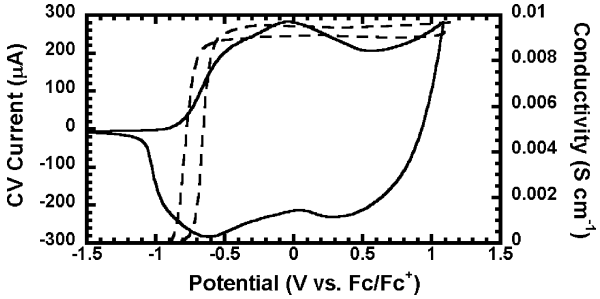

Figure 8. Cyclic voltammogram (−) at 100 mV/s and in situ conductivity (- -) of **p-1d.** The same in situ conductivity conditions for **p-1c** were used for **p-1d**.

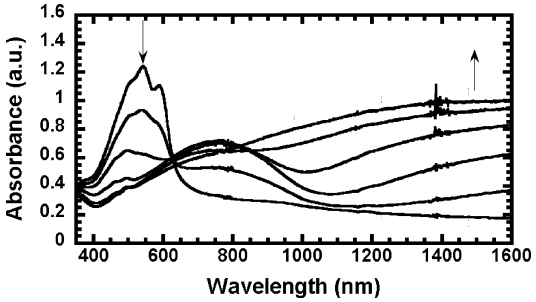

Figure 9. Spectroelectrochemistry of **p-1d** grown onto ITO with potential changes from −0.8 to 0.2 V in 0.2 V intervals.

electroactivity. The observation of two reduction waves is also consistent with this assertion. The in situ conductivity of **p-1c** had only one point of conductivity change and remained high well past the potential region of the wave in the CV. This type of conductivity profile, with large regions of uniformly high conductivity, resembles the conductivity profiles of fully π-conjugated polymers.[28] This result suggests that the redox matching of the metal and organic oxidations produces a polymer with a highly charge delocalized conductive state. The absolute conductivity of **p-1c** was only higher by a factor of 2 than that of the nonmatched polymer (**p-1a**).

The absorption spectrum of **p-1c** in its neutral state (neutral $\lambda_{max} = 572$ nm with a slight shoulder at 586) is significantly red shifted from those of **p-1a** and **p-1b**, as shown in Figure 7. This effect is typical of EDOT substitution in polythiophene.[35] The changes in the UV−vis absorption spectrum of **p-1c** occurred over a smaller potential window (−0.5 to 0.1 V) than the potential window needed for the corresponding changes in the spectroelectrochemistry of **p-1a** (−0.4 to 0.8 V). This decrease of the potential window was consistent with the single broad oxidation in the CV of **p-1c**. At potentials from −0.3 to −0.1 V, a broad absorption at intermediate wavelengths, $\lambda_{max} \approx 780$ nm, is observed, and at higher potentials (−0.1 to 0.1 V), a featureless extremely broad absorption at longer wavelengths dominates the spectrum.

The EDOT homologue of **p-1b** is **p-1d**. As expected, **p-1d**'s onset of electroactivity, as shown in Figure 8, is at a lower potential than **p-1b**'s. Similar to our comparisons of **p-1b** with **p-1a**, **p-1d** displays a larger separation between oxidation and reduction peaks than **p-1c** (0.58 for **p-1d** vs ∼0.29 V for **p-1c**). The in situ conductivity of **p-1d** had a similar profile to the in situ conductivity of **p-1c** in that the profile had only one point of conductivity change and displayed a large window of high conductivity. In contrast to the in situ conductivity of **p-1b**, there was no local minimum in the conductivity profile of **p-1d**. The effects of the length of the thiophene groups are less pronounced than for **p-1b** and **p-1a**; the difference in the absolute conductivities of **p-1d** and **p-1c** is not significant.

In accord with our comparisons of **p-1c** to **p-1a**, the spectroelectrochemistry of **p-1d** was red shifted relative to that of **p-1b**. The neutral absorption of **p-1d** displays $\lambda_{max} = 537$ nm with shoulders at 503 and 590 nm, as shown in Figure 9, and intermediate-wavelength absorptions ($\lambda_{max} \approx 770$ nm) were observed at potentials corresponding to the $Fe^{II/III}$ redox couple, from −0.6 to −0.2 V. Similar to the spectroelectrochemistry of **p-1c**, a broad featureless absorption at longer wavelengths was observed as the polymer was oxidized at higher potentials (−0.2 to 0.2 V). In contrast to the differences observed in the spectroelectrochemistry of **p-1b** relative to that of **p-1a**, there was no red shift of the neutral absorption λ_{max}'s of **p-1d** in comparison to that of **p-1c**. This result was consistent with the comparison of the absolute conductivities of **p-1c** and **p-1d**. It appears that in the case of the EDOT substitution that a difference in the length of the conjugated linker between the metal sites in each polymer does not produce an observable effect in the bulk charge delocalization. However, like the difference in the onset of conductivity for **p-1b** in comparison to the onset for **p-1a**, the onset of conductivity for **p-1d** did occur at a lower potential than **p-1c**'s. A direct comparison of the in situ conductivities of all of the polymers, as shown in Figure 10, demonstrates the lowering of the onset of conductivity by decreasing the length in the conjugated linker between metal sites. It is readily apparent that the onset of conductivity of a polymer with two thiophene units between the azaferrocene sites (**p-1b** and **p-1d**) occurs at a lower potential than does the onset of conductivity of a polymer of the analogous polymer with four thiophene units between azaferrocene units (**p-1a** and **p-1c**). These results suggest that a superexchange mechanism may be responsible for the lowering of these onsets. However, a model study and a Hush analysis are needed to quantify the number of electronic and electrostatic

(35) (a) Groenendaal, L.; Jonas, F.; Freitag, D.; Pielartzik, H.; Reynolds, J. R. *Adv. Mater.* **2000**, *12*, 481. (b) Roncali, J.; Blanchard, P.; Frere, P. *J. Mater. Chem.* **2005**, *15*, 1589.

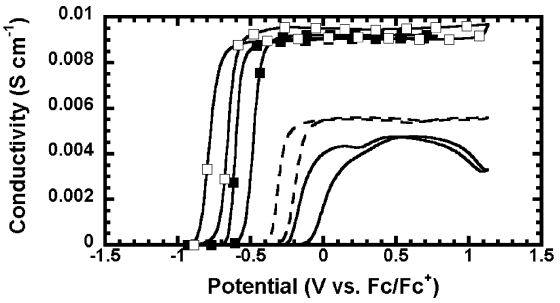

Figure 10. In situ conductivities of **p-1a** (−), **p-1b** (- -), **p-1c** (■), and **p-1d** (□).

contributions to the interaction between the metal centers, but such a study is beyond that the scope of the present investigation.[36]

Conclusions

A series of polythiophene derivatives containing azaferrocene were synthesized. The polymers displayed metal-based redox conductivity. This significant redox conductivity was attributed to the molecular architecture wherein the π-bound metal was attached to a fully π-conjugated polymer backbone. A change in the length of the thiophene section between the azaferrocene units indicated a modification in the redox conductivity mechanism that perhaps involved a superexchange-type mechanism.

Acknowledgment. This research was supported by the U.S. Army through the Institute for Solider Nanotechnology under contract DAAD-19-02-0002 with U.S. Research Office. We thank Dr. Ivory Hills for advice on the synthesis of the azaferrocenes complexes and Dr. Koushik Venkatesan for discussions of organometallic mixed-valance systems.

Supporting Information Available: Crystallographic data of **1a** and XPS data of **p-1a.** This material is available free of charge via the Internet at http://pubs.acs.org.

LA061078H

(36) Sutton, J. E.; Sutton, P. M.; Taube, H. *Inorg. Chem.* **1979**, *18*, 1017.